Optical Engineering

Implementation of uniform diffraction efficiency of partially overlapping holograms in photopolymers based on the photopolymerization of a free radical

Wei Song
Shiquan Tao
Qianli Zhai
Dayong Wang

Implementation of uniform diffraction efficiency of partially overlapping holograms in photopolymers based on the photopolymerization of a free radical

Wei Song
Shiquan Tao
Qianli Zhai
Dayong Wang
Beijing University of Technology
College of Applied Science
Institute of Information Photonics Technology
Room 2103, Pingleyuan 100
Chaoyang District, Beijing 100124, China
E-mail: shqtao@bjut.edu.cn

Abstract. The exposure schedule model for uniform diffraction efficiency is extended to be suitable for the partially overlapping multiplexing method. The proposed model is based on solving an optimization problem. Fifty holograms were multiplexed using the exposure schedule calculated with the extended model. The material used in the experiment is based on the photopolymerization of a free radical. By comparing the intensity of the reconstructed images during recording with that readout after recording, the calculated exposure schedule is verified to be effective to realize the uniform diffraction efficiency for the multiplexing holographic storage. © *The Authors. Published by SPIE under a Creative Commons Attribution 3.0 Unported License. Distribution or reproduction of this work in whole or in part requires full attribution of the original publication, including its DOI.* [DOI: 10.1117/1.OE.52.4.045801]

Subject terms: exposure schedule; holographic storage; photopolymer.

1 Introduction

Holographic storage is a potential data recording technology because of its high storage capacity and fast data rate.[1] Compared with holographic photorefractive crystals, photopolymers are considered to have the most potential material for holographic storage because of their low cost, high diffraction, easy processing, and other advantages.[1–3] There are two kinds of photopolymer holographic recording material based on cationic ring-opening polymerization or the photopolymerization of a free radical.[4,5] In our work, the photopolymer based on the photopolymerization of a free radical is in use. The recording material has been developing and a dual-monomer photopolymer has been introduced. It is dual-wavelength sensitized for increasing the storage density and capacity.[6] According to the previous work,[7] experimental tests had shown that there are usually two advantages of the dual-monomer photopolymer. First, the polymerization efficiencies of the dual-monomer are higher than those of the single-monomer ones, which also provides an easier way to increase the refractive index modulation. Second, the dual-monomer design improves the stability of the material in polymerization due to the combination of the dual monomer with the different physical and chemical property. Besides, the experimental results also have shown that the concentration ratio of POEA and NVC kept stable with few changes or fluctuation in the polymerization, which suggests that the two monomers polymerize independently without any interaction.

The mechanism of holographic recording in photopolymers based on the photopolymerization of a free radical consists of two processes.[8–10] One is the monomer's polymerization caused by the exposure of the interference pattern in holographic recording, which leads to monomer concentration gradient. The other is the diffusion caused by the gradient of monomers, which leads to a refractive index change, so holographic gratings are recorded inside the material. Models were introduced for the dynamics of a single-grating formation in photopolymers taking into account spatial-dependent diffusion of monomers[11] and time-dependent photo-polymerization rate.[12]

In the application of a large-area photopolymer for holographic storage, partially overlapping multiplexing methods, such as spatioangular multiplexing,[13] shift-multiplexing,[14] and polytopic multiplexing,[15] are applied widely. To increase the storage density, it is an effective way to apply the speckle-encoded reference beam generated by a diffuser to the shift-multiplexing method.[16,17] The dynamics of grating formation in the partially overlapping multiple recording is much more complicated including three processes: holographic recording, dark reaction, and uniform postexposure (UPE).[18,19] Different parts of one hologram experience different durations of the three processes.

However, it is very important make diffraction efficiency of all recorded holograms uniform in the application of multiplexed holography. For this purpose, the mechanism of gratings formation involving the influence of sequential recordings should be investigated. An empirical approach was proposed[20] and implemented.[21–23] In this method a six-order polynomial was obtained by fitting experimental data of cumulative index modulation versus cumulative exposure time by recording tens of holograms. With parameters acquired from the fitting data, exposure time of the individual hologram was calculated for uniform diffraction efficiency.[20–23] But several times of recording holograms and fitting calculation are needed to obtain the optimum time schedule realizing uniform diffraction. An experiment conducted to validate the method has been done and shown that the polynomial curve exhibited an anomalous trend in the saturation regime when it was extended from the end time of the experiment with a longer recording time, which implies that the polynomial fit does not reflect the real physical process of multiplexing.[18]

Another method was proposed to identify an optimum exposure schedule for photopolymer materials governed

by the nonlocal polymerization-driven diffusion model.[24] In this model, sufficient time between sequential recordings must be allowed, to wait for full monomer relaxation caused by the diffusion effect. It means that a hologram should not be recorded until the previous one finished its relaxation. However, the relaxation of a monomer often lasts several minutes.[24,25] This is not suitable for dense holographic storage in which a huge number of holograms are required to be written.

We have proposed a simplified model for grating formation in photopolymers based on the first-harmonic diffusion model[18] and extended the work to a calculation model for exposure schedules applicable to holographic recordings with common-volume (e.g., pure angle or wavelength) multiplexing methods in single-monomer photopolymers.[19] In this paper, we extend the simplified model further to be suitable for holographic recording with partially overlapping multiplexing methods, and the effect of dual-monomer is considered. Using the extended model, a time schedule for recording 50 holograms is calculated, and uniform diffraction efficiency is implemented in an experiment of shift multiplexing.

2 Physical Mechanism for Diffraction Efficiency of Gratings in Dual-Monomer Photopolymers

Holograms recorded in single-monomer photopolymers generally experience three processes:[18,19] holographic recording, dark reaction, and postexposure process. The index modulation, Δn, reached during holographic recording is expressed as

$$\Delta n(t) = \Delta n_{\text{SAT}} \left\{ 1 + \frac{\tau_D}{\tau_P} \exp\left[-\left(\frac{1}{\tau_P} + \frac{1}{\tau_D} \right) t \right] \right. \\ \left. - \left(1 + \frac{\tau_D}{\tau_P} \right) \exp\left(-\frac{t}{\tau_P} \right) \right\}, \quad (1)$$

where Δn_{SAT} is the saturation index modulation that is related to the initial monomer concentration, τ_D is the diffusion time constant, and τ_P is the polymerization time constant.

After the exposure stopped at $t = t_w$ the gratings would still grow up for a period based on the diffusion effect, which is referred to as dark reaction. The evolution of index modulation during dark reaction is expressed as

$$\Delta n(t) = \Delta n(t_w) + A \cdot \left[1 - \exp\left(\frac{t_w - t}{\tau_D} \right) \right]. \quad (2)$$

where A is related to the monomer concentration at $t = t_w$.

Furthermore, the dynamics of refractive index modulation of a grating under UPE after a short holographic recording can be expressed as

$$\Delta n(t) = \Delta n(t_w) + C \left\{ 1 - \exp\left[-\left(\frac{1}{\tau_p} + \frac{1}{\tau_D} \right) \cdot (t - t_e) \right] \right\}, \quad (3)$$

where t_e is the start time of the postexposure process, and C is related to the monomer concentration at $t = t_e$. In multiple

recordings, the effect of a sequential recording on an existing grating can be considered as UPE. Usually, the saturation refraction index of UPE and dark reaction is much lower than that of a holographic recording.[3,4]

On the other hand, in the dual-monomer photopolymer, the two kinds of monomers participate in the polymerization independently,[7] without influence on each other, during holographic writing, dark reaction, and postexposure. In this way, the final refractive index modulation of the grating, $\Delta n(t)$), should be expressed as

$$\Delta n(t) = \Delta n_1(t) + \Delta n_2(t), \quad (4)$$

where Δn_1 is the refractive index modulation of one monomer (M1), and Δn_2 is that of another one (M2). The development of both refractive index modulation Δn_1 and Δn_2 follows Eqs. (1)–(3) and can be calculated with the polymerization time constant τ_{P1}, τ_{P2}, the diffusion time constant τ_{D1}, τ_{D2}, and the saturation index modulation Δn_{SAT1}, Δn_{SAT2}, respectively. These parameters can be obtained by the data-fitting method with dark reaction and holographic writing experiments. The composition of the material for this paper are detailed in Table 1.

In the holographic writing and dark reaction experiments, the laser source is the Verdi™-V5 Diode-Pumped Lasers from Coherent Company. The wavelength of recording beams is 532 nm. The total exposure intensity is 15 μW/mm^2, and the intensity ratio of object beam to reference beam is 1:1. The angle between the two recording beams is 45 deg, and the thickness of the material is 500 μm. According to Eqs. (2) and (4), the constants τ_{D1} and τ_{D2} can be obtained directly with the experiment results of dark reaction by data-fitting processing. Then, according to Eqs. (1) and (4), the constants Δn_{SAT1}, Δn_{SAT2}, τ_{P1} and τ_{P2}

Table 1 Composition of the recording material.[a]

Components	Material	Weight percentage (%)
Monomer1	NVC	12.9
Monomer2	POEA	25.2
Binder	BGE	46.5
Chain transfer agent	MMT	0.8
Dye	BTCP	0.012
Photoinitiator	HABI	0.8
Curing agent	TETA	12.4
Dissolvent	DMF	1.4

[a]NVC: N-Vinyl carbazole; POEA: 2-phenoxyethyl ester; BGE: 1,4-butanediol diglycidyl ether; BTCP: 2,5-bis(2,3,6,7-tetrahydro-1H,5H-pyrido[3,2,1-ij]quinolin-9-ylmethylene)-cyclopentanone; HABI: 1,1,2,2-bis(o-chlorophenyl)-4,4,5,5-tetraphenyl-bisimidazole;TETA: triethylenetetramine; DMF: dimethylformamide; MMT: 4-ylmethyl-4H-1,2,4-triazole-3-thiol.
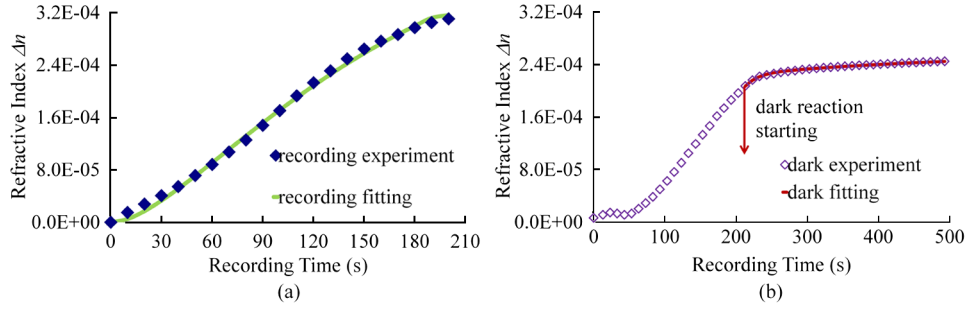
Fig. 1 Experiment and fitting curves of (a) holographic recording and (b) dark reaction.

can be obtained with the holographic recording and the obtained constants τ_{D1} and τ_{D2}. The calculation of data-fitting processing are solved by the computer. The experimental and fitting curves are shown in Fig. 1, and the correlation coefficient is 0.999.

The fitted constants are $\tau_{P1} = 319.32$ s, $\tau_{D1} = 95.15$ s, $\tau_{P2} = 18.76$ s, $\tau_{D2} = 44.15$ s, $\Delta n_{SAT1} = 4.19 \times 10^{-4}$ and $\Delta n_{SAT2} = 3.62 \times 10^{-5}$, $A_1 = 3.51 \times 10^{-5}$ and $A_2 = 1.88 \times 10^{-5}$ for the photopolymer currently used in the experiment. The subscript 1 stands for the solid monomer NVC, and subscript 2 stands for the liquid monomer POEA here. The saturation diffraction efficiency of the material is 70.13%.

Considering the order of magnitude of Δn is generally less than 10^{-4}, in the condition of small index modulation, diffraction efficiency η is propotional to the square of refractive index Δn:

$$\eta \propto \Delta n^2. \tag{5}$$

Equations (1)–(5) together with all necessary parameters fitted from experimental data constitute the fundamentals of our exposure schedule model.

3 Exposure Schedule Model for Partially Overlapping Multiplexing

Take a shift multiplexing recording process for an example, the scheme is demonstrated in Fig. 2 for realizing uniform diffraction efficiency with partially overlapping multiplexing. As Fig. 2(a) shows, the shift interval is δ. Every hologram is divided into r zones, $r = d/\delta.r$ is also defined as the degree of multiplexing, and d is the size of a single
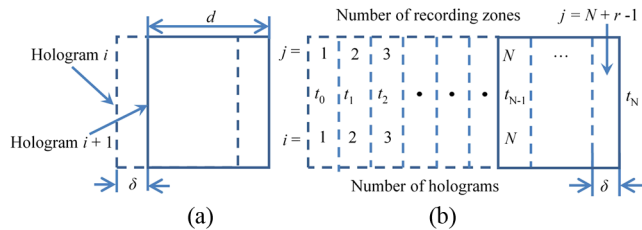

Fig. 2 The scheme of shift multiplexing, (a) for the i'th and $i + 1$'th holograms, (b) for N holograms, i: the sequence number of holograms, $i = 1, 2, 3, \ldots, N$; j: the sequence number of the separated zones, $j = 1, 2, 3, \ldots, i + r - 1$; t_{i-1}: starting time for recording the i'th hologram and t_N: the final ending time.

hologram. In this way, as Fig. 2(b) shows, the whole recording area for total N holograms marked by i is divided into $N + r - 1$ zones marked by j. The total recording time is t_N, $t_N = T$. And for recording the i'th hologram, the recording time is from t_{i-1} to t_i.

The scheme shown in Fig. 2 can depict the situation of every zone in the holographic storage. Generally, each zone experiences holographic recording, UPE, and dark reaction sequentially, but some characteristics are found out in the three processes. For the holographic recording process, the initial monomer concentration in the zones $1 \leq j \leq r$ is different from that in the zones $r < j \leq N + r - 1$ because the latter experiences pre-exposure before recording begins. For the UPE and dark reaction processes, because the other holograms are overlapping with the N'th hologram in the zones $N + 1 \leq j \leq N + r - 1$, there is no dark reaction, but the UPE lasts to the end in these zones.

According to the discussion above, the whole holographic storage can be divided into three different ranges of zone number j, $1 \leq j \leq r$, $r + 1 \leq j \leq N$, and $N + 1 \leq j \leq N + r - 1$. Having investigated the dynamics of index modulation in each zone carefully and through somewhat tedious derivation, we obtained for each range a special mathematical expression for the contribution of the j'th zone to the refractive index modulation of the i'th hologram, Δn_{ij}. In the first range, the contribution of monomer M1 to Δn_{ij}, $\Delta n_{ij}^{(1)}$, can be written as:

$$
\begin{aligned}
\Delta n_{ij}^{(1)}(T) = &\Delta n_{SAT1} \left\{ \exp\left(-\frac{t_{i-1}}{\tau_{P1}}\right) - \left(1 + \frac{\tau_{D1}}{\tau_{P1}}\right) \exp\left(-\frac{t_i}{\tau_{P1}}\right) \right. \\
&\left. + \frac{\tau_{D1}}{\tau_{P1}} \exp\left(\frac{t_{i-1}}{\tau_{D1}}\right) \exp\left[-\left(\frac{1}{\tau_{P1}} + \frac{1}{\tau_{D1}}\right) t_i\right] \right\} \\
&+ \frac{\tau_{D1}(\tau_{P1} + \tau_{D1})}{\tau_{P1}^2} \Delta n_{SAT1} \exp\left[-\left(\frac{1}{\tau_{P1}} + \frac{1}{\tau_{D1}}\right) t_j\right] \\
&\times \left[\exp\left(\frac{t_j}{\tau_{D1}}\right) - \exp\left(\frac{t_{i-1}}{\tau_{D1}}\right)\right]\left[1 - \exp\left(\frac{t_j - T}{\tau_{D1}}\right)\right] \\
&+ \frac{\tau_{D1}}{\tau_{P1}} \Delta n_{SAT1} \exp\left[-\left(\frac{1}{\tau_{P1}} + \frac{1}{\tau_{D1}}\right) t_i\right] \cdot \left[\exp\left(\frac{t_i}{\tau_{D1}}\right)\right. \\
&\left. - \exp\left(\frac{t_{i-1}}{\tau_{D1}}\right)\right]\left\{1 - \exp\left[-\left(\frac{1}{\tau_{D1}} + \frac{1}{\tau_{P1}}\right)(t_j - t_i)\right]\right\}, \\
&(1 \leq j \cong r). \tag{6}
\end{aligned}
$$

In the intermediate range,

$$
\begin{aligned}
\Delta n_{ij}^{(1)}(T) = {} & \Delta n_{\mathrm{SAT1}} \exp\left(\frac{t_{j-r}}{\tau_{P1}}\right) \left\{ \exp\left(-\frac{t_{i-1}}{\tau_{P1}}\right) - \left(1+\frac{\tau_{D1}}{\tau_{P1}}\right) \right. \\
& \times \exp\left(-\frac{t_i}{\tau_{P1}}\right) + \frac{\tau_{D1}}{\tau_{P1}}\exp\left(\frac{t_{i-1}}{\tau_{D1}}\right) \\
& \left. \times \exp\left[-\left(\frac{1}{\tau_{P1}}+\frac{1}{\tau_{D1}}\right)t_i\right] \right\} + \frac{\tau_{D1}(\tau_{P1}+\tau_{D1})}{\tau_{P1}^2}\Delta n_{\mathrm{SAT1}} \\
& \times \exp\left(\frac{t_{j-r}}{\tau_{P1}}\right)\exp\left[-\left(\frac{1}{\tau_{P1}}+\frac{1}{\tau_{D1}}\right)t_j\right]\left[\exp\left(\frac{t_j}{\tau_{D1}}\right)\right. \\
& \left. -\exp\left(\frac{t_{i-1}}{\tau_{D1}}\right)\right]\left[1-\exp\left(\frac{t_j-T}{\tau_{D1}}\right)\right]+\frac{\tau_{D1}}{\tau_{P1}}\Delta n_{\mathrm{SAT1}} \\
& \times \exp\left(\frac{t_{j-r}}{\tau_{P1}}\right)\exp\left[-\left(\frac{1}{\tau_{P1}}+\frac{1}{\tau_{D1}}\right)t_i\right]\cdot\left[\exp\left(\frac{t_i}{\tau_{D1}}\right)\right. \\
& \left. -\exp\left(\frac{t_{i-1}}{\tau_{D1}}\right)\right]\left\{1-\exp\left[-\left(\frac{1}{\tau_{D1}}+\frac{1}{\tau_{P1}}\right)(t_j-t_i)\right]\right\}, \\
& (r<j\leq N),
\end{aligned}
\tag{7}
$$

and in the last range

$$
\begin{aligned}
\Delta n_{ij}^{(1)}(T) = {} & \Delta n_{\mathrm{SAT1}} \exp\left(\frac{t_{j-r}}{\tau_{P1}}\right) \left\{ \exp\left(-\frac{t_{i-1}}{\tau_{P1}}\right) - \left(1+\frac{\tau_{D1}}{\tau_{P1}}\right) \right. \\
& \times \exp\left(-\frac{t_i}{\tau_{P1}}\right) + \frac{\tau_{D1}}{\tau_{P1}}\exp\left(\frac{t_{i-1}}{\tau_{D1}}\right) \\
& \left. \times \exp\left[-\left(\frac{1}{\tau_{P1}}+\frac{1}{\tau_{D1}}\right)t_i\right] \right\} + \frac{\tau_{D1}}{\tau_{P1}}\Delta n_{\mathrm{SAT1}} \\
& \times \exp\left(\frac{t_{j-r}}{\tau_{P1}}\right)\exp\left[-\left(\frac{1}{\tau_{P1}}+\frac{1}{\tau_{D1}}\right)t_i\right]\left[\exp\left(\frac{t_i}{\tau_{D1}}\right)\right. \\
& \left. -\exp\left(\frac{t_{i-1}}{\tau_{D1}}\right)\right]\left\{1-\exp\left[-\left(\frac{1}{\tau_{D1}}+\frac{1}{\tau_{P1}}\right)(T-t_i)\right]\right\}, \\
& (N<j\cong N+r-1).
\end{aligned}
\tag{8}
$$

By changing the subscript "1" to "2" in Eqs. (6)–(8), we obtain the correspondent expressions for monomer M2. And then, using Eqs. (4) and (5), the contribution of the j'th zone to the diffraction efficiency of the i'th hologram can be obtained. The derivation of Eqs. (6)–(8) will be detailed in the Appendix.

Our purpose is to calculate an exposure schedule, $t_1 - t_0, t_2 - t_1, \ldots, t_N - t_{N-1}$, $(t_N = T)$, following which the diffraction efficiencies of total N holograms are uniform. Furthermore, the uniform diffraction efficiency should be as high as possible. This calculation for the maximum average is equivalent to the following optimization problem:

$$
\text{Max} \sum_{j=i}^{i+r-1} [\Delta n_1(i,j) + \Delta n_2(i,j)]^2, \qquad i = 1, 2, 3, \ldots, N
\tag{9}
$$

with a restriction

$$
\sum_{j=i}^{i+r-1} [\Delta n_1(i,j) + \Delta n_2(i,j)]^2 = C_1 \qquad i = 1, 2, 3, \ldots, N,
\tag{10}
$$

where C_1 is a constant. Equation (10) means the diffraction efficiency of the i'th hologram occupying r zones from $j = i$ to $j = i + r - 1$ is equal to a common value C_1, so the diffraction efficiencies can be uniform. Additionally, there is another restriction according to the physical condition, that is, the refractive index modulation of each zone should not exceed the permitted range of the material:

$$
\sum_{i=j-r+1}^{j} [\Delta n_1(i,j) + \Delta n_2(i,j)] \leq C_2(\Delta n_{\mathrm{SAT1}} + \Delta n_{\mathrm{SAT2}}),
$$
$$
i = 1, 2, 3, \ldots, N.
\tag{11}
$$

The left hand of Eq. (11) represents the refractive index modulation of the j'th zone overlapped by r holograms from $i = j - r + 1$ to $i = j$, and the coefficient $C_2(C_2 \leq 1)$ in the right hand is an adjustable controlling constant, but it does not need to make each zone's refractive index modulation also uniform.

The optimization model can be solved numerically by the computer. The routing time for calculating an exposure schedule is typically 6.2 s. Using the fitted parameters obtained from Fig. 1, and taking the controlling constant $C_2 = 0.5$ and multiplexing degree $r = 6$, an exposure schedule for 51 holograms was calculated and shown in Fig. 3. The total exposure time is $T = 531$ s. The exposure time for the sequentially recorded holograms is rising smoothly except for the 51st. It is reasonable because the diffraction efficiencies of the former 50 holograms are compensated in dark reaction and UPE processes after holographic recording. But the 51st hologram only experiences the holographic recording process without any additional compensation, so the exposure time for recording the 51st hologram is much longer than the others.

4 Experiment of Multiplexing Storage

To verify the calculated schedule, a multiplexing experiment with shift multiplexing has been done, and the setup is shown in Fig. 4. The laser source and other experiment conditions are the same as those in the holographic recording and dark reaction experiments mentioned above except the intensity ratio of object beam to reference beam is 1:2 in the multiplexing experiment. The object beam is modulated by the spatial light modulator (SLM). An image is located to the SLM, making the object to be recorded. Then, through
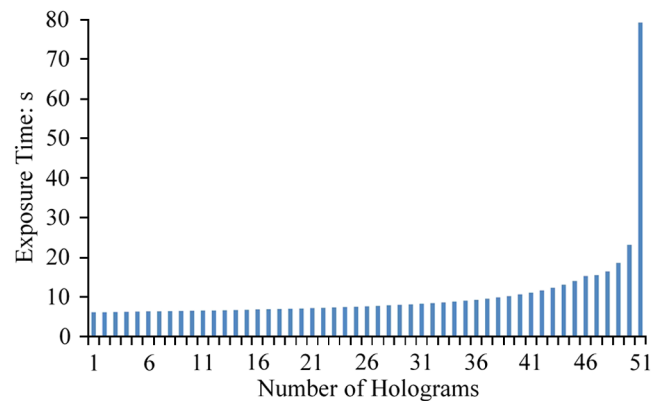

Fig. 3 The calculated exposure schedule for 51 hologram recordings in dual-monomer photopolymer.
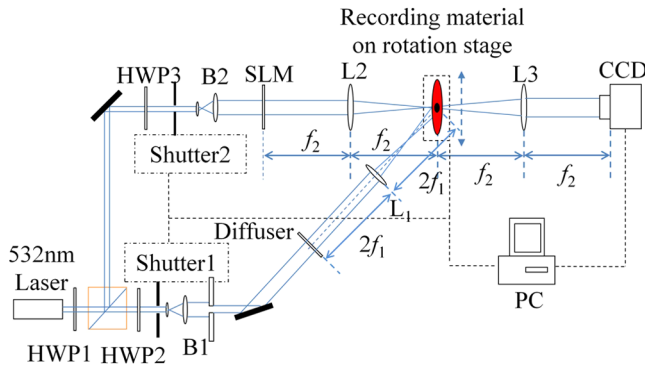
Fig. 4 Experiment setup. f_1, f_2, f_3 are focal lengths of lenses $L1, L2, L3$, respectively. B: beam expander and collimation; HWP: half wave plate; L: lens.

Lens L2, the Fourier transform of the object is obtained on the plane of recording media. The reference beam, modulated by a diffuser, is imaged by inserting Lens L1, to the plane of recording media, so that the reference wave is phase-only modulated. The diffuser is a speckle phase shifter with the speckle size of 50 μm. The shifting interval δ is 0.25 mm leading to a multiplexing degree $r = 6$, since the hologram spot on the material is 1.5 mm.

Using the calculated exposure schedule shown in Fig. 3, 51 holograms were recorded in a dual-monomer photopolymer disc. The actual total recording time was 570 s, a little longer than the calculated one due to the time consumption of the stage rotating and program routine.

The reconstructed images are captured by a CCD camera whose automatic gain and background light control function

is closed, so the gray scale of the image can reflect the image intensity. To monitor the multiplexing recording process, each hologram was read out immediately after its recording finished, and after the 51 hologram recordings finished, all the holograms were reconstructed once again.

The reconstructed image of the 51st hologram is degraded due to excessive exposure for its overlong recording time; nevertheless, others were reconstructed successfully. So, the calculated exposure schedule shown in Fig. 3 is actually suitable for recording 50 holograms. The reconstructed images for holograms No. 23 and No. 46 are shown in Fig. 5. Although the noise increased, as shown in Fig. 5(c) and 5(d), the intensity of the two reconstructed images became closer than in the monitoring process, as shown in Fig. 5(a) and 5(b). It is noticed that the reconstructed images after recording are darker than those in monitoring because the scattering noise gratings rise during the whole recording process, which makes the transmittance of the whole recording area fall down.[26,27] Therefore, all the recorded holograms are influenced. Similarly, other reconstructed images after recording are also darker than those in monitoring.

In order to estimate the experimental result quantitatively, we use the average gray scale of an image as a measure of its intensity, which is proportional to its diffraction efficiency. The gray scale of every image is normalized by that of the first one, which is referred to as normalized intensity. The normalized intensity of the reconstructed images read out immediately after recording, and the final reconstructed images are shown in Fig. 6. The curve for the images read out immediately is rising all the time as shown in Fig. 6(a). It is reasonable because the more recording time is offered, the higher diffraction efficiency is gotten before the saturation.
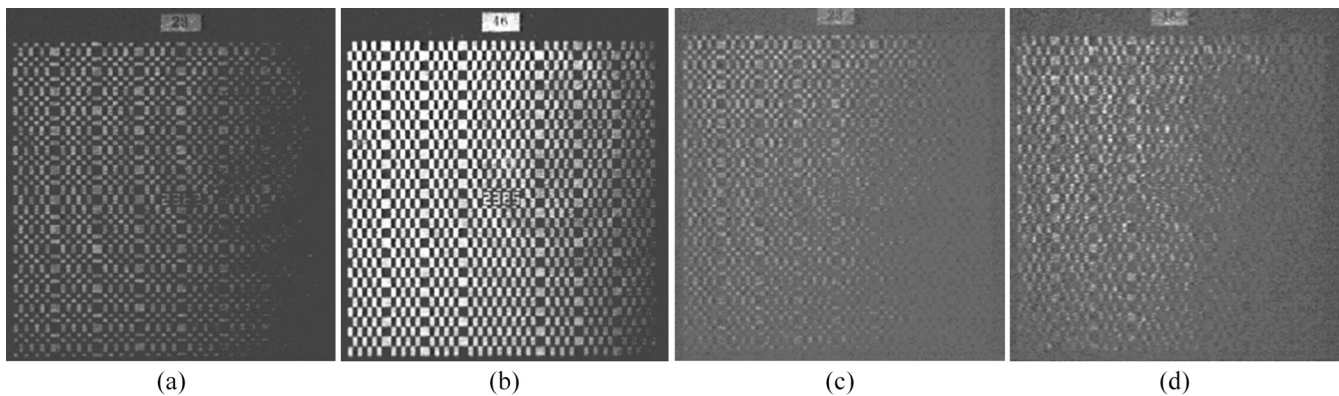

(a)   (b)   (c)   (d)

Fig. 5 The reconstructed images for No. 23 and No. 46 hologram. (a) No. 23 in monitoring, (b) No. 46 in monitoring, (c) No. 23 after recording process, (d) No. 46 after recording process.
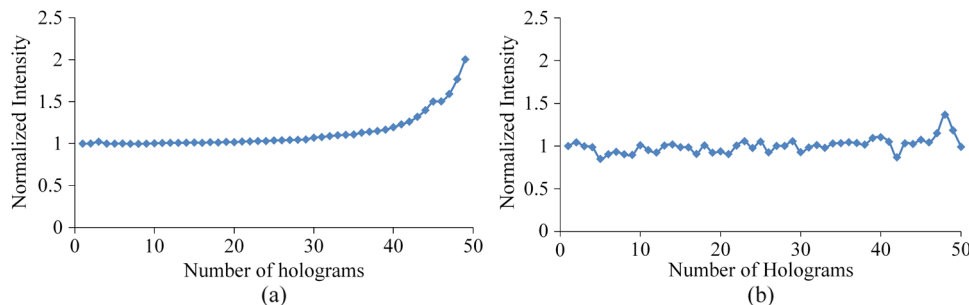

Fig. 6 The normalized intensity of the reconstructed images, (a) for the monitoring images and (b) for the final reconstructed images.

In contrast, the curve for the final ones, as Fig. 6(b) shows, is quite close to a straight line. It means the previous recorded holograms in relatively low diffraction efficiency were compensated by dark reaction and UPE for different time following the calculated schedule in Fig. 3, and finally, diffraction efficiency of all the recorded holograms is more uniform.

5 Conclusion

We extended the exposure schedule model of uniform diffraction efficiency in a single-monomer photopolymer to that in dual monomers with partially overlapping multiplexing method and proposed an optimization algorithm to calculate the schedule. The extended model is validated by a preliminary experiment. By using a shift-multiplexing method for 50 holograms in a dual-monomer photopolymer material with the calculated exposure schedule, the intensity of the final reconstructed images became fairly uniform. The proposed model is surely suitable for other partially overlapping multiplexing, such as the phase-shift multiplexing method.[28]

Additionally, it is noticed that the final reconstructed images are influenced by the scattering noise gratings and become darker than those in monitoring. We will discuss it and raise the quality of the recorded holograms in our future work.

Appendix: The Derivation of Eqs. (6)–(8)

We have proposed a simplified model[18,19] from fundamental principles of monomer diffusion and photo-polymerization.[12]

$$\frac{du_0(t)}{dt} = -\frac{1}{\tau_P} u_0(t) \tag{12}$$

$$\frac{du_1(t)}{dt} = \frac{1}{\tau_P}\left[\frac{1}{2}mu_0(t) - u_1(t)\right] - \frac{u_1(t)}{\tau_D}, \tag{13}$$

where $u_0(t)$ stands for the average of momomer concentration, $u_1(t)$ is the amplitude of monomer concentration modulated distribution. m is the modulation of interference fringes. By solving Eq. (13), $u_0(t)$ is expressed as:

$$u_0(t) = \exp\left(-\frac{t}{\tau_P}\right), \qquad t \in [0, T]. \tag{14}$$

The refractive index modulation is calculated by Eq. (15) (Ref. 3):

$$\frac{d\Delta n}{dt} = \frac{C_n}{\tau_D} u_1(t), \tag{15}$$

where C_n is a proportional constant.

For the holographic recording, $u_0(t)$ is related to the start time of recording. According to the physical model for partially overlapping multiplexing shown in Fig. 2, the start time is t_{j-r} in the range of $j > r$, so Eq. (14) is modified as follows:

$$u_{0j}(t) = \begin{cases} U \exp\left(-\frac{t}{\tau_P}\right), & j \in [1, r] \\ U \exp\left(-\frac{t-t_{j-r}}{\tau_P}\right), & j \in (r, N+r-1] \end{cases}. \tag{16}$$

where U is the monomer concentration before holographic recording.

It is noticed that $u_{ij1}(t_{i-1})$ is 0 because holographic recording is just starting at the time t_{i-1} for the i'th hologram. With this conditon, by Eqs. (13) and (16), $u_{1ij}(t)$ in different range of j can be gotten in the range $t \in [t_{i-1}, t]$.

$$u_{1ij}(t) = \frac{m\tau_D U}{2\tau_P} \exp\left[-\left(\frac{1}{\tau_P}+\frac{1}{\tau_D}\right)t\right] \cdot \left[\exp\left(\frac{t}{\tau_D}\right) - \exp\left(\frac{t_{i-1}}{\tau_D}\right)\right], \qquad j \in [1, r] \tag{17}$$

$$u_{1ij}(t) = \frac{m\tau_D U}{2\tau_P}\exp\left(\frac{t_{j-r}}{\tau_P}\right)\exp\left[-\left(\frac{1}{\tau_P}+\frac{1}{\tau_D}\right)t\right] \cdot \left[\exp\left(\frac{t}{\tau_D}\right) - \exp\left(\frac{t_{i-1}}{\tau_D}\right)\right], \qquad j \in (r, N+r-1]. \tag{18}$$

Then, with Eqs. (15) and (17) or Eqs. (15) and (19), the refractive index modulation in the recoding process can be depicted as:

$$\Delta n_{ij}(t_i) - \Delta n_{ij}(t_{i-1})$$
$$= \Delta n_{\text{SAT}}\left\{\begin{array}{l} \exp\left(-\frac{t_{i-1}}{\tau_P}\right) - \left(1+\frac{\tau_D}{\tau_P}\right)\exp\left(-\frac{t_i}{\tau_P}\right)+ \\ \frac{\tau_D}{\tau_P}\exp\left(\frac{t_{i-1}}{\tau_D}\right)\exp\left[-\left(\frac{1}{\tau_P}+\frac{1}{\tau_D}\right)t_i\right] \end{array}\right\},$$
$$j \in [1, r] \tag{19}$$

$$\Delta n_{ij}(t_i) - \Delta n_{ij}(t_{i-1})$$
$$= \Delta n_{\text{SAT}}\exp\left(\frac{t_{j-r}}{\tau_P}\right)\left\{\begin{array}{l} \exp\left(-\frac{t_{i-1}}{\tau_P}\right) - \left(1+\frac{\tau_D}{\tau_P}\right)\exp\left(-\frac{t_i}{\tau_P}\right)+ \\ \frac{\tau_D}{\tau_P}\exp\left(\frac{t_{i-1}}{\tau_D}\right)\exp\left[-\left(\frac{1}{\tau_P}+\frac{1}{\tau_D}\right)t_i\right] \end{array}\right\},$$
$$j \in (r, N+r-1], \tag{20}$$

where Δn_{SAT} is expressed as

$$\Delta n_{\text{SAT}} = \frac{C_n m\tau_P U}{2(\tau_P+\tau_D)} \tag{21}$$

Also, because holographic recording for the i'th hologram is not happening before the time t_{i-1}, the refractive index modulation attributed by the i'th hologram $\Delta n_{ij}(t_{i-1})$ is 0.

For the UPE, the modulaton of the interference fringes m is 0. And Eq. (13) is modified as:

$$\frac{du_{1ij}(t)}{dt} = -\left[\frac{1}{\tau_P}+\frac{1}{\tau_D}\right]u_{1ij}(t) \tag{22}$$

then $u_{1ij}(t)$ can be gotten in the range $t \in [t_i, t]$.

$$u_{1ij}(t) = u_{1ij}(t_i)\exp\left[-\left(\frac{1}{\tau_D}+\frac{1}{\tau_P}\right)(t-t_i)\right], \tag{23}$$

where $u_{1ij}(t_i)$ can be gotten by Eqs. (17) and (18) in a different range of j at the time t_i, the end of the holographic recording. Then, with Eqs. (15) and (23), the refractive index modulation in UPE process can be gotten in the range $t \in [t_i, t_j]$ in the condition of $j \cong N$, or in the range $\in [t_i, T]$ in the conditon of $j > N$ according to the model shown in Fig. 2.

$$\Delta n_{ij}(t_j) - \Delta n_{ij}(t_i)$$
$$= \begin{cases} u_{1ij}(t_i) \dfrac{C_n \tau_P}{\tau_D + \tau_P} \left\{ 1 - \exp\left[-\left(\dfrac{1}{\tau_D} + \dfrac{1}{\tau_P} \right)(t_j - t_i) \right] \right\}, & j \leq N \\ u_{1ij}(t_i) \dfrac{C_n \tau_P}{\tau_D + \tau_P} \left\{ 1 - \exp\left[-\left(\dfrac{1}{\tau_D} + \dfrac{1}{\tau_P} \right)(T - t_i) \right] \right\}, & j > N \end{cases}.$$

(24)

As discussed above, considering the different expression of $u_{1ij}(t)$ shown in Eqs. (17) and (18) in a different range of j at the time t_i, the index modulation in UPE process is divided into three parts:

$$\Delta n_{ij}(t_j) - \Delta n_{ij}(t_i)$$
$$= \frac{\tau_D}{\tau_P} \Delta n_{\text{SAT}} \exp\left[-\left(\frac{1}{\tau_P} + \frac{1}{\tau_D} \right) t_i \right] \cdot \left[\exp\left(\frac{t_i}{\tau_D} \right) \right.$$
$$\left. - \exp\left(\frac{t_{i-1}}{\tau_D} \right) \right] \times \left\{ 1 - \exp\left[-\left(\frac{1}{\tau_D} + \frac{1}{\tau_P} \right)(t_j - t_i) \right] \right\},$$
$$j \cong r$$

(25)

$$\Delta n_{ij}(t_j) - \Delta n_{ij}(t_i)$$
$$= \frac{\tau_D}{\tau_P} \Delta n_{\text{SAT}} \exp\left(\frac{t_{j-r}}{\tau_P} \right) \exp\left[-\left(\frac{1}{\tau_P} + \frac{1}{\tau_D} \right) t_i \right] \cdot \left[\exp\left(\frac{t_i}{\tau_D} \right) \right.$$
$$\left. - \exp\left(\frac{t_{i-1}}{\tau_D} \right) \right] \times \left\{ 1 - \exp\left[-\left(\frac{1}{\tau_D} + \frac{1}{\tau_P} \right)(t_j - t_i) \right] \right\},$$
$$r < j \leq N$$

(26)

$$\Delta n_{ij}(T) - \Delta n_{ij}(t_i)$$
$$= \frac{\tau_D}{\tau_P} \Delta n_{\text{SAT}} \exp\left(\frac{t_{j-r}}{\tau_P} \right) \exp\left[-\left(\frac{1}{\tau_P} + \frac{1}{\tau_D} \right) t_i \right] \cdot \left[\exp\left(\frac{t_i}{\tau_D} \right) \right.$$
$$\left. - \exp\left(\frac{t_{i-1}}{\tau_D} \right) \right] \times \left\{ 1 - \exp\left[-\left(\frac{1}{\tau_D} + \frac{1}{\tau_P} \right)(T - t_i) \right] \right\},$$
$$j > N.$$

(27)

For the dark reaction, the terms $1/\tau_P$ and m are 0 because of no exposure in this process. So Eq. (13) is modified as:

$$\frac{du_{1ij}(t)}{dt} = -\frac{u_{1ij}(t)}{\tau_D},$$

(28)

then $u_{1ij}(t)$ can be gotten in the range $t \in [t_j, t]$.

$$u_{1ij}(t) = u_{1ij}(t_j) \exp\left(\frac{t_j - t}{\tau_D} \right),$$

(29)

where $u_{1ij}(t_j)$ can be obtained by Eqs. (17) and (24) in the range $j \in [1, r]$, or Eqs. (18) and (24) in the range $j \in$

$(r, N + r - 1]$ at the time t_j, the end of UPE. Then, with Eqs. (15) and (32), the refractive index modulation in dark reaction process can be gotten in the range $t \in [t_j, T]$, according to the model shown in Fig. 2. Besides, it is noticed that there is no dark reaction in the range of $N \cong j \cong N + r - 1$, so the expression of the index modulation in dark reaction is also divided into three parts:

$$\Delta n_{ij}(T) - \Delta n_{ij}(t_j) = \frac{\tau_D(\tau_P + \tau_D)}{\tau_P^2} \Delta n_{\text{SAT}} \exp\left[-\left(\frac{1}{\tau_P} + \frac{1}{\tau_D} \right) t_j \right]$$
$$\times \left[\exp\left(\frac{t_j}{\tau_D} \right) - \exp\left(\frac{t_{i-1}}{\tau_D} \right) \right]$$
$$\times \left[1 - \exp\left(\frac{t_j - T}{\tau_D} \right) \right], \quad j \leq r$$

(30)

$$\Delta n_{ij}(T) - \Delta n_{ij}(t_j) = \frac{\tau_D(\tau_P + \tau_D)}{\tau_P^2} \Delta n_{SAT} \exp\left(\frac{t_{j-r}}{\tau_P} \right)$$
$$\times \exp\left[-\left(\frac{1}{\tau_P} + \frac{1}{\tau_D} \right) t_j \right] \cdot \left[\exp\left(\frac{t_j}{\tau_D} \right) \right.$$
$$\left. - \exp\left(\frac{t_{i-1}}{\tau_D} \right) \right] \left[1 - \exp\left(\frac{t_j - T}{\tau_D} \right) \right],$$
$$r < j \leq N$$

(31)

$$\Delta n_{ij}(T) - \Delta n_{ij}(t_j) = 0, \qquad N < j \cong N + r - 1.$$

(32)

Then, by changing the representation "τ_P" to "τ_{P1}" and "τ_D" to "τ_{D1}", the expression of the contribution of monomer M1 to Δn_{ij}, $\Delta n_{ij}^{(1)}$, in the range of $1 \leq j \cong r$ as shown in Eq. (6), can be obtained by adding Eqs. (19), (25), and (30). The expression of Eq. (7) in the range of $r < j \cong N$ can be obtained by adding Eqs. (20), (26), and (31). And the expression of Eq. (8) can be obtained by adding Eqs. (20), (27), and (32).

References

1. H. J. Coufal, D. Psaltis, and G. Sincerbox, *Holographic Data Storage*, pp. 106–109, Springer, New York (2000).
2. J. R. Lawrence, F. T. O'Neill, and J. T. Sheridan, "Photopolymer holographic recording material," *Optik* **112**(10), 449–463 (2001).
3. L. Hesselink, S. S. Orlov, and M. C. Bashaw, "Holographic data storage systems," *Proc. IEEE* **92**(8), 1231–1280 (2004).
4. D. A. Waldman et al., "Cationic ring-opening photopolymerimization methods for volume hologram recording," *Proc. SPIE* **2689**, 127–141 (1996).
5. J. Guo et al., "Study of photosensitizer diffusion in a photopolymer material for holographic applications," *Opt. Eng.* **50**(1), 015801 (2011).
6. S. Tao, Y. Zhao, and Y. Wan, "Dual-wavelength sensitized photopolymer for holographic data storage," *Jpn. J. Appl. Phys.* **49**, 08KD01 (2010).
7. M. Shi et al., "Effect of dual monomers' ratio on properties of photopolymers for holographic storage," *Imag. Sci. Photochem.* **26**(5), 410–416 (2008).

8. L. Carretero et al., "Theoretical and experimental study of the bleaching of a dye in a film-polymerization process," *Appl. Opt.* **37**(20), 4496–4499 (1998).
9. S. Liu et al., "Extended model of the photoinitiation mechanisms in photopolymer materials," *J. Appl. Phys.* **106**(10), 104911 (2009).
10. M. R. Gleeson et al., "Non-local photo-polymerization kinetics including multiple termination mechanisms and dark reactions: part II. Experimental validation," *J. Opt. Soc. Am. B* **26**(9), 1746–1754 (2009).
11. G. H. Zhao and P. Mouroulis "Diffusion-model of hologram formation in dry photopolymer materials," *J. Mod. Opt.* **41**(10), 1929–1939 (1994).
12. S. Piazzolla and B. K. Jenkins, "First-harmonic diffusion model for holographic grating formation in photopolymers," *J. Opt. Soc. Am. B* **17**(7), 1147–1157 (2000).
13. S. Tao, D. R. Slevich, and J. E. Midwinter, "Spatio-angular multiplexed storage of 750 holograms in an Fe:LiNbO3 crystal," *Opt. Lett.* **18**(11), 912–914 (1993).
14. G. J. Steckman, A. Pu, and D. Psaltis, "Storage density of shift-multiplexed holographic memory," *Appl. Opt.* **40**(20), 3387–3394 (2001).
15. K. Anderson and K. Curtis, "Polytopic multiplexing," *Opt. Lett.* **29**(12), 1402–1404 (2004).
16. Q. He et al., "Dynamic speckle multiplexing scheme in volume holographic data storage and its realization," *Opt. Lett.* **11**(4), 366–370 (2003).
17. M. Miura et al., "Three-dimensional shift selectivity in reflection-type holographic disk memory with speckle shift recording," *Appl. Opt.* **46**(9), 1460–1466 (2007).
18. T. Zhang et al., "Research on the dark diffusion transient for a blue-green sensitized holographic photopolymer material," *Proc. SPIE* **6796**, 67961M (2008).
19. Q. Zhai, S. Tao, and X. Song, "Investigation on mechanism of multiple holographic recording with uniform diffraction efficiency in photopolymers," *Opt. Express* **17**(13), 10871–10880 (2009).
20. A. Pu, K. Curtis, and D. Psaltis, "Exposure schedule for multiplexing holograms in photopolymer films," *Opt. Eng.* **35**(10), 2824–2829 (1996).
21. E. Fernández et al., "Comparison of peristrophic multiplexing and a combination of angular and peristrophic holographic multiplexing in a thick PVA/acrylamide photopolymer for data storage," *Appl. Opt.* **46**(22), 5368–5373 (2007).
22. M. Ortuno et al., "Hologram multiplexing in acrylamide hydrophilic photopolymers," *Opt. Commun.* **281**(6), 1354–1357 (2008).
23. S. Gallego et al., "Analysis of monomer diffusion in depth in photopolymer materials," *Opt. Commun.* **274**(1), 43–49 (2007).
24. J. T. Sheridan, F. T. O'Neill, and J. V. Kelly, "Holographic data storage: optimized scheduling using the nonlocal polymerization-driven diffusion model," *J. Opt. Soc. Am.* **21**(8), 1443–1451 (2004).
25. J. V. Kelly et al., "Optimized scheduling technique for holographic data storage," *Proc. SPIE* **6335**, 63350J (2006).
26. J. A. Frantz, R. K. Kostuk, and D. A. Waldman, "Model of noise-grating selectivity in volume holographic recording materials by use of Monte Carlo simulations," *J. Opt. Soc. Am. A* **21**(3), 378–387 (2004).
27. S. Tao et al., "Scattering noise properties of holographic photopolymers by means of real-time transmittance analysis," *Chin. Phys. Lett.* **25**(8), 2896–2899 (2008).
28. S. Honma, S. Muto, and A. Okamoto, "Shift-phase code multiplexing technique for holographic memories and optical interconnection," *Proc. SPIE* **6832**, 68322P (2007).

Wei Song received BS and MSc degrees in physics in 2007 and 2010 from Beijing University of Technology, China. Now he is a PhD candidate in optical engineering in the Beijing University of Technology. His main research interests are optical information processing and holographic data storage.

Shiquan Tao graduated from the Radio and Electronics Department of Peking University, China, in 1969, and obtained her MSc and PhD degrees from Soochow University, China, in 1981 and from University of London, United Kingdom, in 1993, respectively. She is currently a professor in the College of Applied Science, Beijing University of Technology, China. Her main research interests are optical information processing and holographic data storage.

Qianli Zhai received BS and PhD degrees in physics in 2005 and 2011 from Beijing University of Technology, China. Now he is working in the Patent Examination Cooperation Center of the Patent Office, China.

Dayong Wang received his BS in optical engineering in 1989 from Huazhong University of Science and Technology, Wuhan, China, and his PhD in physics in 1994 from Xi'an Institute of Optics and Fine Mechanics, Chinese Academy of Sciences. From 1994 to 1996 he worked as a postdoctor in Xidian University, China. In 1996 he joined the Department of Applied Physics, Beijing University of Technology (BJUT). From 1998 to 2000, he worked in the Weizmann Institute of Science, Israel, as a visiting scientist. Since 2000, he has been a professor in the College of Applied Sciences, BJUT. His research interests include optical information processing, optical storage, holography, and diffractive optical elements. He is a member of COS, SPIE, and OSA.